# MODELLING THE BOND BETWEEN CONCRETE AND REINFORCING STEEL IN FIRE

by Zhaohui Huang

Department of Civil and Structural Engineering, The University of Sheffield, Sheffield, S1 3JD, UK.

(Tel: +44(0)114 2225710, Fax: +44(0)114 2225700, Email: z.huang@sheffield.ac.uk)

## ABSTRACT

A non-linear procedure is presented for modelling the bond characteristic between concrete and reinforcing steel for reinforced concrete structures in fire. The accuracy and reliability of the model are demonstrated by the analysis of one pull-out test and one beam test at ambient temperature and four full-scale beams tested under two fire conditions. The model is clearly capable of predicting the response of reinforced concrete members and structures in fire with acceptable accuracy. The bond-link element has been found to have good computational stability and efficiency for 3D analysis of reinforced concrete structures in fires. It is shown that the bond condition between the concrete and reinforcing steel bar has important influence on the fire resistance of reinforced concrete structures, especially when the temperature of the reinforcing steel bar is high (more than 500°C). Hence, the current assumption of the perfect bond condition for analysis of reinforced concrete structures under fire conditions is unconservative.


**Key-words:** bond characteristic; bond-link element; fire resistance of concrete structures; finite element analysis.

# 1. Introduction

The behaviour of structures exposed to fire is usually described in terms of the concept of fire resistance, which is the period of time under exposure to a standard fire time-temperature curve at which some prescribed form of limiting behaviour occurs. In performance-based design this limiting behaviour may be defined either as real structural collapse or as a failure of integrity which would allow fire-spread to occur, but is more usually defined in terms of a deflection limit. The most recent design codes, EN 1992-1-2 [1] and EN 1994-1-2 [2] have taken a step towards full performance-based design by allowing designers to treat fire as one of the basic design limit states, taking account of:

- Non-uniform heating due to partial protection, which may be inherent in the framing system or specially applied,

- The level of loading at the fire limit state, using partial safety factors lower than those used for ultimate limit states, because of the relative improbability of such accidental combinations,

- Realistic stress-strain characteristics of structural materials at elevated temperatures.

The main limitation of these codified approaches is that they are based on the behaviour under test of isolated simply supported members, usually heated according to the standard ISO834 [3] time-temperature curve. In real buildings structural elements form part of a continuous assembly, and building fires often remain localised, with the fire-affected region of the structure being subject to significant restraint from cooler areas surrounding it. The real behaviour of these structural elements can therefore be very different from that indicated by standard furnace tests. An additional encouragement towards this end is the increasing volume of evidence from full-scale fire tests in building structures [4] that members which form part of a connected frame do not behave similarly to their performance in isolation in furnace tests. The interaction between the key effects (differential heating of cross-sections, material degradation as temperatures rise, and the capacity for load-sharing and restraint to thermal expansion provided by cool surrounding structure) makes

2

the real behaviour extremely complex. If such interactions are to be used by designers in specifying fire protection strategies as part of an integrated limit state structural design process rather than as an adjunct to it, then this can not practically be based on large-scale testing because of the extremely high implicit costs. It is therefore becoming increasingly important that software models be developed to enable the behaviour of such structures to be predicted with sufficient accuracy under fire conditions.

In recent years a number of numerical models have been developed to represent the behaviour of reinforced concrete structures in fire [5-10], but none of these have taken the influence of the bond characteristic between concrete and reinforcing steel into account. In a number of previous research projects for modelling the bond characteristic between concrete and reinforcing steel at ambient temperature [11-21], two common types of models have been used. The first one is to use the so called bond-link element which connect concrete element and reinforcing steel element at the nodes [11-13]. Normally, the link element has no physical dimensions, for example, the two connected nodes from two different type elements have the same coordinates at the beginning of the analysis. The second approach is to use a 'bond-zone connect' element [14-19]. In this approach, the characteristics of the contact surface between concrete and reinforcing steel is represented by a material law which considers the properties of the bond zone. In this model it is assumed that the contact element provides a continuous connection between concrete and reinforcing steel. Hence, more fine mesh is needed within the bond zone area in order to achieve reasonable accuracy. In comparison, for modelling global structural behaviour of reinforced concrete structures the bond-link element provides a reasonable compromise between accuracy and computational efficiency.

In recent years, a robust 3-noded beam-column element has been developed at the University of Sheffield for 3D modelling of steel, composite and reinforced concrete frames under fire conditions [22, 23]. In this model both material and geometric non-linearities are considered. The cross-section of the beam-column element is divided into a matrix of segments, and each segment may have different material, temperature and mechanical properties. The complications of structural

3

behaviour in fire conditions, such as thermal expansion, degradation of stress-strain curves, failure of concrete segments by cracking and crushing, and yielding of reinforcement segments, are included. In this beam-column element, it is possible to offset the nodes by pre-determined distances, the elements can easily be combined with shell or plate elements to model reinforced concrete or composite structures in fire. Of course, a problem with these developments is that they ignore the influence of bond between concrete and reinforcing steel on the structural behaviour of the reinforced concrete structures. Hence, the main objective of this paper is to develop a bond-link element to model the interaction between plain concrete and reinforcing steel. The element developed permits modelling of full, partial and even zero interaction between the concrete and reinforcing steel within the reinforced concrete structures. Also, the bond-link element can be used to model interaction between concrete and reinforcing steel for reinforced concrete slabs in fire.

## 2. Non-linear procedure

As shown in Fig. 1(a) a reinforced concrete beam is modelled as an assembly of finite plain concrete, reinforcing steel bar and bond-link elements. It is assumed that the nodes of these different types of element are defined in a common reference axis. For modelling of reinforced concrete frame structures the reference axis is normally assumed to coincide with the central axis of the cross-section of the beam and column members (see Fig. 1 (a)). Its location is fixed throughout the analysis. Hence, in Fig. 1(a) the plain concrete beam element is represented as 3-noded beam-column element with zero offset, and the reinforcing steel bar element is modelled as 3-noded beam-column element with the offsets of $\Delta y$ and $\Delta z$, respectively. A bond-link element makes the connection between a plain concrete element node and a reinforcing steel bar element node. That means one 3-noded steel bar element needs only three bond-link elements in order to make the connection with the plain concrete element. Therefore, the model proposed here is very computationally effective.

## 2.1 Plain concrete beam-column and reinforcing steel bar elements

As shown in the Fig. 2, the cross-sections of the plain concrete beam and steel bar elements are divided into a matrix of segments in order to consider the variation of temperature and material properties within the cross-sections. In this model a "void segment" is introduced to represent the volume occupied by reinforcing steel bar within the cross-section of plain concrete elements (see Fig. 2(b)). It is assumed that the "void segment" has zero mechanical strength and stiffness. The detailed formulations of the 3-noded beam-column element and the constitutive modelling of concrete and steel at elevated temperatures have been presented previously [22, 23]. For the constitutive modelling of the materials, the compressive and tensile strengths of concrete, yield strength of reinforcing steel, Young's modules of concrete and steel are all reduced at elevated temperatures following the models specified in Eurocode 2 [1].

## 2.2 Concrete-steel bond-link element

For modelling the interaction between the reinforcing steel and the concrete within the reinforced concrete structural members it is necessary to develop a bond element to link the two components. The details of connection of the three elements are shown in Fig. 1(a). The reinforcing steel is represented as equivalent beam element. The bond element shown in Fig. 1(b) is a specialised two-noded element of zero length, which has three translational degrees of freedom $u, v, w$ and three rotational degrees of freedom $\theta_x, \theta_y, \theta_z$ at each node, where $x, y, z$ are local coordinates of reinforcing steel element in which $x$ is the direction of longitudinal axis of the reinforcing steel element. It is assumed that the slip between reinforcing steel and concrete is related only to the longitudinal axis direction ($x$-direction). Hence, at ambient temperature the bonding force between the concrete and reinforcing steel bar for the bond element is obtained from the following equation

$$F_x = A\tau_b \qquad (1)$$

Where,

$F_x$ = the bond force between the reinforcing steel bar and concrete for the bond element;

$A = $ the contact-area between the reinforcing steel bar and concrete for the bond element, that is, $A = UL$, where $U$ is the perimeter of the steel bar and $L$ is the length of the steel bar which contributes to the node connected by the bond element;

$\tau_b = $ the average bond stress between concrete and reinforcing steel bar related to the bond element.

The average bond stress, $\tau_b$, can be calculated using an empirical bond stress-slip relationship defined in the CEB-FIP Model Code 90 [24]. That is,

$$\tau_b = \tau_{max} \left( \frac{s}{s_1} \right)^{\alpha} \quad for \ 0 \le s \le s_1 \tag{2}$$

$$\tau_b = \tau_{max} \qquad for \ s_1 < s \le s_2 \tag{3}$$

$$\tau_b = \tau_{max} - \left( \tau_{max} - \tau_f \right) \left( \frac{s - s_2}{s_3 - s_2} \right) \quad for \ s_2 < s \le s_3 \tag{4}$$

$$\tau_b = \tau_f \qquad for \ s_3 < s \tag{5}$$

where,

$\tau_{max} = $ maximum bond stress;

$s = $ the slip between concrete and reinforcing steel.

Fig. 3 shows the relationship between the average bond stress $\tau_b$ and the slip $s$. The parameters of $\tau_{max}$, $s_1$, $s_2$ and $s_3$ in above equations can be found from Reference 24 for ribbed and smooth reinforcing steel bars, respectively. In order to consider the influence of different grades of concrete on the average bond stress, the maximum bond stress, $\tau_{max}$, is directly related to the compressive strength of the concrete used [24].

Previous research indicated that the bond stress-slip relationship depends on a considerable number of influencing factors: such as type of steel bar (ribbed or smooth); roughness (related rib area), concrete strength, position and orientation of the bar during casting, state of stress, boundary

conditions and concrete cover. Therefore the bond stress-slip curve, represented by above equations can be considered as a statistical mean curve, applicable as an average formulation for a broad range of cases [24].

*Bond strength at elevated temperatures*

Investigations into the bond strength between concrete and reinforcing steel at room temperature have been carried out over many years. Comparatively few experiments have, however, been carried out to investigate the effects of high temperatures on the bond characteristics. Bazant and Kaplan [25] summarised some tested results which are shown in Fig. 4 and some broad conclusions were drawn as:

- Bond strength is reduced as temperature increases and the reduction rate is greater compared to concrete strengths.

- The percentage reduction of bond strength for ribbed bars at elevated temperatures is generally less than for plain round steel bars.

- Differences in the diameters of plain bars and deformed bars had little effect on the strength reduction of the bond.

- The experimental procedure used affects the results of bond tests at high temperatures.

- The type of aggregate in the concrete affects the bond strength at elevated temperatures.

- The smaller the concrete cover, the greater is the reduction in bond strength.

Due to the complexity of bond characterization at elevated temperatures, as first order approximation, simplified bi-linear and tri-linear models, as shown in Fig. 4 are proposed here to calculate the bond strengths of ribbed and smooth bars at elevated temperatures, respectively.

For ribbed bars, the bond strength reduction at high temperatures can be represented as,

$$\tau_{max,T} = \tau_{max,20}\left(1.0 - \frac{0.22}{360}(T-20)\right) \qquad for \ 20 \ ^0C \le T \le 380 \ ^0C \qquad (6)$$

$$\tau_{max,T} = \tau_{max,20}\left(0.78 - \frac{0.75}{270}(T-380)\right) \qquad for \ 380 \ ^0C < T \le 650 \ ^0C \qquad (7)$$

7

$$\tau_{max,T} = 0.03\,\tau_{max,20} \qquad\qquad\qquad\qquad \textit{for } 650\ ^0C < T \qquad\qquad\qquad (8)$$

For smooth bars, the bond strength reduction at high temperatures can be determined by,

$$\tau_{max,T} = \tau_{max,20}\left(1.0 - \frac{0.35}{180}(T - 20)\right) \qquad \textit{for } 20\ ^0C \le T \le 200\ ^0C \qquad\qquad (9)$$

$$\tau_{max,T} = \tau_{max,20}\left(0.65 - \frac{0.27}{200}(T - 200)\right) \qquad \textit{for } 200\ ^0C < T \le 400\ ^0C \qquad\qquad (10)$$

$$\tau_{max,T} = \tau_{max,20}\left(0.38 - \frac{0.35}{140}(T - 400)\right) \qquad \textit{for } 400\ ^0C < T \le 540\ ^0C \qquad\qquad (11)$$

$$\tau_{max,T} = 0.03\,\tau_{max,20} \qquad\qquad\qquad\qquad \textit{for } 540\ ^0C < T \qquad\qquad\qquad (12)$$

Of course, the above model can be improved if more comprehensive test data is available.

The computer program *Vulcan* [22, 23] has recently been extended to include a two-dimensional non-linear finite element procedure to predict the temperature distributions within the cross-sections of structural members subject to given fire time-temperature regimes. This is largely based on previous work [26] by the author. The thermal properties of the steel and concrete are assumed to change with temperature, and the influence of moisture initially held within the concrete has been taken into account. In this analysis the thermal properties given in EN 1992-1-2 [1] for concrete and steel have been adopted.

*Stiffness matrix of concrete-steel bond-link element*

For simplicity it is assumed that there is no coupling of effects due to different degrees of freedom for the bond-link element. This means that the nodal deformation and force of each degree of freedom are determined only by the stiffness and displacement related to that degree of freedom, respectively. This simplified approach has been successfully used in the previous research [27]. Hence in the local co-ordinate, referenced to the reinforcing steel bar element, the nodal force increment vector, $\{\Delta F\}$ of the element can be related to its nodal displacement increment vector $\{\Delta u\}$ as

$$
\begin{Bmatrix}
\Delta F_{x,1} \\
\Delta F_{y,1} \\
\Delta F_{z,1} \\
\Delta M_{x,1} \\
\Delta M_{y,1} \\
\Delta M_{z,1} \\
\Delta F_{x,2} \\
\Delta F_{y,2} \\
\Delta F_{z,2} \\
\Delta M_{x,2} \\
\Delta M_{y,2} \\
\Delta M_{z,2}
\end{Bmatrix}
=
\begin{bmatrix}
k_1 & 0 & 0 & 0 & 0 & 0 & -k_1 & 0 & 0 & 0 & 0 & 0 \\
0 & k_2 & 0 & 0 & 0 & 0 & 0 & -k_2 & 0 & 0 & 0 & 0 \\
0 & 0 & k_3 & 0 & 0 & 0 & 0 & 0 & -k_3 & 0 & 0 & 0 \\
0 & 0 & 0 & k_4 & 0 & 0 & 0 & 0 & 0 & -k_4 & 0 & 0 \\
0 & 0 & 0 & 0 & k_5 & 0 & 0 & 0 & 0 & 0 & -k_5 & 0 \\
0 & 0 & 0 & 0 & 0 & k_6 & 0 & 0 & 0 & 0 & 0 & -k_6 \\
-k_1 & 0 & 0 & 0 & 0 & 0 & k_1 & 0 & 0 & 0 & 0 & 0 \\
0 & -k_2 & 0 & 0 & 0 & 0 & 0 & k_2 & 0 & 0 & 0 & 0 \\
0 & 0 & -k_3 & 0 & 0 & 0 & 0 & 0 & k_3 & 0 & 0 & 0 \\
0 & 0 & 0 & -k_4 & 0 & 0 & 0 & 0 & 0 & k_4 & 0 & 0 \\
0 & 0 & 0 & 0 & -k_5 & 0 & 0 & 0 & 0 & 0 & k_5 & 0 \\
0 & 0 & 0 & 0 & 0 & -k_6 & 0 & 0 & 0 & 0 & 0 & k_6
\end{bmatrix}
\begin{Bmatrix}
\Delta u_1 \\
\Delta v_1 \\
\Delta w_1 \\
\Delta \theta_{x,1} \\
\Delta \theta_{y,1} \\
\Delta \theta_{z,1} \\
\Delta u_2 \\
\Delta v_2 \\
\Delta w_2 \\
\Delta \theta_{x,2} \\
\Delta \theta_{y,2} \\
\Delta \theta_{z,2}
\end{Bmatrix}
\qquad (13)
$$

For reinforcing steel bars, apart from the relative slip along the longitudinal axis direction ($x$-direction) between concrete and steel bars the concrete prevents relative movement of reinforcing bars in other directions. It is therefore reasonable to assume that common nodes of the concrete and reinforcing bar elements have identical rotations and movements in $y$ and $z$ directions. Hence, in this model $k_2$, $k_3$, $k_4$, $k_5$, $k_6$ in Eq. (13) are assumed to have infinite magnitude. However, the above model can be extended to take into account the influence of concrete spalling. That is, when the surrounding concrete at steel bar spalls the bond between concrete and steel is lost. Therefore, $k_1, k_2$, $k_3$, $k_4$, $k_5$, $k_6$ in Eq. (13) become zero.

Coefficient $k_1$ is the tangent stiffness coefficients of the bond connector which can be determined from the experimental load-slip relationship in Eq. (1):

$$
k_1 = \frac{dF_x}{ds} = A\frac{d\tau_b}{ds} \qquad (14)
$$

Using Eqs. (2) to (5), the following equations can be obtained:

$$
k_1 = \frac{A\tau_{max}}{s_1}\left(\frac{s}{s_1}\right)^{\alpha-1} \qquad for\ 0\leq s\leq s_1 \qquad (15)
$$

$$
k_1 = 0.0 \qquad for\ s_1 < s\leq s_2 \qquad (16)
$$

9

$$k_1 = -\left(\frac{\tau_{max} - \tau_f}{s_3 - s_2}\right) \qquad for \ s_2 < s \leq s_3 \tag{17}$$

$$k_1 = 0.0 \qquad for \ s_3 < s \tag{18}$$

Using incremental analysis, the increment of bond force $\Delta F_x$ can be related to the increment of slip, $\Delta s$ by the tangent stiffness relationship

$$\Delta F_x = k_1 \Delta s \tag{19}$$

in which

$$\Delta s = \Delta u_1 - \Delta u_2 \tag{20}$$

where $\Delta u_1$ and $\Delta u_2$ are the increments of displacement in the direction of $\Delta F_x$ at the nodes 1 and 2 of the bond-link element, respectively.

The bond-link element permits the modelling of full, partial and zero interaction at the interface between the concrete and reinforcing steel bars. By using Eqs. (6) to (12) the bond characteristic between concrete and reinforcing steel bars at elevated temperatures can be modelled.

In the non-linear incremental/iterative analysis procedure, increments of slip are summed to obtain the total slip at any load level. The bond force corresponding to total slip is determined from Eq. (19), and the tangent stiffness of the element for the next iteration is calculated using Eqs. (14) to (18).

The above developments have been incorporated into the computer program *Vulcan* [22, 23] in order to model the structural behaviour of reinforced concrete structures under fire conditions. This software has been developed at the University of Sheffield for 3D modelling of steel, composite and reinforced concrete structures in fire. The total loading or temperature rise for which the response of the structure is to be traced is divided into a number of steps. It is assumed that changes in the loads or temperatures occur only at the beginning or end of a step. During any step the external loads and temperatures in the segments of all elements are assumed to remain unchanged.

## 3. Validations

In order to validate the model presented above a series of validations was conducted in which both ambient and fire conditions were used. Also in all validation cases both material and geometric non-linearities were considered. In this section one pull-out test; one reinforced concrete beam at ambient temperature and four reinforced concrete beams tested in fires were analysed. The results were compared with the corresponding experimental data to demonstrate the robustness and accuracy of the model.

In order to validate the effectiveness of the model developed above, in which the reinforcing steel bar was represented by three-noded beam elements with off-set, subjected to very large deformation, an artificial simply supported 4$m$ reinforced concrete beam subjected to point load at mid-span was analysed first. The details of the beam are shown in Fig. 5. The compressive strength of concrete is 35 MPa and yield strength of reinforcing steel is 600 MPa. In this validation both material and geometrical non-linearities were considered. Within the cross-section there are two tensile and two compressive reinforcing steel bars. The beam was modelled firstly by using reinforced concrete elements without the bond-link element. This means that a perfect bond condition between concrete and reinforcing steel bar was assumed. Secondly, the beam was analysed again as an assembly of plain concrete, reinforcing steel bar and bond-link elements in which the bar element was assumed never to fail with very large stiffness, $k_1 = 10^{12} \, MPa$, to represent the perfect bond condition. This approach was also adopted for modelling fully composite action of shear connectors for the composite beam [27]. It was found that the model had very good numerical stability. In this analysis four types of reinforcing steel bar elements at different locations within the cross section were used to represent tensile and compressive reinforcing steel within the cross-section. As shown in Fig. 6 the finite element mesh comprised of a total of 4 three-noded plain concrete elements, 4 x 4 three-noded reinforcing steel bar elements with off-set. Therefore, there were 9 nodes for plain concrete elements and 36 nodes for steel bar elements. Each concrete node was connected to four steel nodes

11

through 4 bond-link elements. Hence, a total of 36 two-noded bond-link elements was used in the analysis. All nodes were defined at a common reference axis at the centre of the cross-section. The vertical and horizontal displacements of the beam at mid-span position are shown in Fig. 7. It is evident that almost identical results (even for very large deformation) were achieved by both models. Hence, the two displacement curves predicted with and without bond-link element are overlapped each other as shown in the figure. The results confirmed the robustness and accuracy of using a 3-noded beam-column element with off-set to model reinforcing steel bars.

## 3.1 Pull-out test at ambient temperature

A pull-out test was conducted by Viwathanatepa et al [28] at University of California, Berkeley in 1979. The test specimen is an anchored #8 ribbed bar in a well confined block of 635mm width (equivalent to an anchorage length of 25 bar diameters). The specimen was subjected to a monotonic pull-out loading condition and under displacement control at one end only. The tested material properties of concrete and steel (the concrete compressive strength, $f_c = 32.4\,MPa$; the yield strength of the reinforcing steel, $f_y = 468.4\,MPa$) were used as input data for the modelling. Same as the above case (see Fig. 6) the finite element mesh of this test includes a total of 4 three-noded plain concrete elements, 1 x 4 three-noded reinforcing steel bar elements with zero off-set. Hence, there were 9 nodes for plain concrete elements and 9 nodes for steel bar elements. Each concrete node was connected to one steel node through one bond-link element. Therefore, a total of 9 two-noded bond-link elements was employed in the analysis. The comparisons of the predicted and tested stress distribution within the anchored reinforcing steel bar at three end-stress (end pull-out force divided by cross-section area of steel bar) levels are shown in Fig. 8. It is clear that reasonable agreements between the model's predictions and test data were achieved. It is interesting to note that the stress in the reinforcing steel bar decreases sharply away from the loaded end. The stress at the position of the middle of the bar is about less than 25% of the stress at the ends. Fig. 9 gives the predicted evolution of the bond stress field for the different loaded end slips. Due to the

tested total pull-out-curve not being available, Fig. 10 presents the predicted end-slips against total pull-out forces for the test. The results indicate that the strength of the bond between concrete and reinforcing steel plays a very important role in controlling the load capacity of reinforced concrete structural members.

## 3.2 Simply supported reinforced concrete beam at ambient temperature

In order to demonstrate the capability of the current model for simulating the bending deformation of the reinforced concrete structural members, a beam tested by Gaston et al [29] was used for the validation. The details of the tested beam are shown in Fig. 11. The area of reinforcing steel bar is 257.3 mm$^2$. The tested concrete strength, $f_c = 31.7\,MPa$ and steel yield strength, $f_c = 317.2\,MPa$, were used for the analysis. By applying symmetry only half a beam was modelled. Based on the same principle of model discretisation described above a total of 4 three-noded plain concrete elements, 1 x 4 three-noded reinforcing steel bar elements with 119.9 mm off-set from the central reference axis and 9 bond-link elements were employed.

Fig. 12 shows the predicted load-centre deflection curves with different bond conditions together with the test results. It is evident that the effect of bond characteristic on the structural behaviour of the beam is significant. The initial discrepancy between the modelling and the test is due to the fact that in the modelling the reinforced concrete beam was assumed to be perfectly intact before the loading, however, in the reality the beam was subjected to certain degree of cracking due to the concrete shrinkage before the loading. It is clear that the proposed model which includes bond-slip effect produced a good agreement with the test data. The predicted failure load for the beam was about 6% higher than the test data. This may be caused by the small difference between the real location of reinforcing steel bar in the tested beam and the location used (see Fig. 11) in the modelling.

13

## 3.3 Fire tests of reinforced concrete beams

Lin *et al*. [30] conducted a series of fire tests on normal-strength reinforced concrete beams with ribbed reinforcing steel bar for which two heating curves, the ASTM fire and Short Duration High Intensity (SDHI) fire, were adopted. In this validation four beams, designated Beams 1, 3, 5 and 6, were modelled. Beams 1 and 3 were heated using the ASTM fire and Beams 5 and 6 were subjected to the SDHI fire.

The first step of the analysis is to perform a thermal analysis on the beams modelled. As shown in Fig. 13 the arrangement of reinforcing steel bars in the tested beam varied along the length of the beam. In this study for the thermal analysis the cross-sections of the beams were segmented into 28 rows and 16 columns and the total number of the concrete and steel segments was 448 (28x16). The reinforcing steel bars were represented as steel segments within the cross-section and varied along the length of the beam. Predicted temperature history of each concrete and steel segment was used as thermal input data for the structural analysis. Hence, in the structural analysis the same segmentation of the cross-section of the beam was used for plain concrete elements in which the volumes occupied by the reinforcing steel bars were represented as void segments. The temperatures of the reinforcing steel bars were represented by the temperatures of the steel segments at related locations within the cross-section considered. By using the same principle of model discretisation described previously, a total of 10 three-noded plain concrete elements with 448 segments; 48 three-noded reinforcing steel bar elements with off-set from the central reference axis of the beam and 104 bond-link elements were employed for modelling the whole beam.

Fig. 13 provides details of Beams No. 1 3, 5 and 6. The load $P$ was kept constant at 44.48 kN during each fire test, although the cantilever force $P_0$ varied as the test progressed. The measured values of $P_0$ for the beams and the test values of material properties at room temperature were used for the modelling. Thermal analysis was conducted to predict temperature histories within the beam cross-sections. As shown in Fig. 13, there are four layers of main reinforcing steel within the

14

cross-sections. In presenting the results of the thermal analysis, the reinforcing steel layers are denoted in sequence from bottom to top as Layers 1 to 4. The predicted temperature histories of the main reinforcing steel layers for Beams 1 and 5, which were subsequently used for structural analysis, are shown in Figs 14 and 15, together with those test results which are available. It is evident that reasonable agreement has been achieved between test and prediction.

As shown in Fig. 13 the beam continues to span over the right-hand support. Hence, the maximum vertical deflection of the beam was at the position closed to the left-hand support. In the following figures the predicted and measured maximum deflections of the beams were referenced to the deflections at the position of 3500mm away from the right-hand continue support. The predictions of the current model with different bond conditions, for Beam 1 are shown in Fig. 16, together with test results. It is evident that the bond characteristic between concrete and reinforcing steel bar has a very significant effect on the fire resistance of the beam. For the smooth bar case the fire resistance of the beam is about 95min. However, by using the ribbed bar (which is real case) about 225min fire resistance can be achieved for the same beam. The current model with ribbed bar bond condition produced reasonable agreement with test results, especially concerning the failure time. Figs 17 and 18 show the comparisons of the maximum deflection and deflection at the position of the cantilever-end of the Beam 3 (see Fig. 13) for different bond conditions. Once again the bond condition has a significant influence on the structural behaviour of the beam. In this case the fire resistance of the beam with the smooth bar is only 50% of the beam with ribbed bar. It is interesting to see that the influence of bond condition is more significant over the continuous support compared to the mid-span areas of the beam. This can be clearly demonstrated by using the deflections at the cantilever-end of the beam in which the test data was not available (see Fig. 18).

The results of modelling Beams 5 and 6 are shown in Figs 19 to 21. It can be seen that the affect of bond condition is relative small compared to the Beams 1 and 3. This is due to the fact that those beams were subjected to Short Duration High Intensity (SDHI) fire. Therefore, the maximum temperatures of the reinforcing steel bars were less than 400°C (see Fig. 15). However, Fig. 21

clearly shows the influence of bond condition on the behaviour of Beam 6. It is evident that the fire resistance of the beams with smooth bar is very poor compared with the performance of tested beams in which the ribbed bar was used. Concerning the complexity and uncertainness of the full scale fire test the predictions of current model agree reasonable well with the test results for the 4 beams.

## 4. Conclusions

A non-linear procedure for modelling the bond characteristic between concrete and reinforcing steel for reinforced concrete structures in fire has been presented. The proposed model is simple and efficient, and has easily been incorporated into the *Vulcan* program for three-dimensional modelling of reinforced concrete buildings subjected to fire. In spite of the lack of test data on the actual bond stress-slip characteristics at elevated temperatures, the model has been shown to detect the major structural effects and to produce logical results. The bond-link element has been found to have good computational stability and efficiency for 3D analysis of reinforced concrete structures in fire. The analysis conducted in this research indicates that the bond condition between concrete and reinforcing steel bar has important influence on the fire resistance of the reinforced concrete structures, especially when the temperature of the reinforcing steel bar is high (more than 500°C). For smooth reinforcing steel bars the assumption of the perfect bond condition for the analysis of reinforced concrete structures under fire conditions is unconservative. Hence, the bond characteristic between concrete and reinforcing steel should need to be considered for the fire resistance design of reinforced concrete structures using smooth bars. In terms of fire engineering design the failure of bond between concrete and reinforcing steel, particularly in beams with little or no continuity, may be the key criterion for fire resistance, but this clearly needs further parametric studies before general rules can be proposed.

**REFERENCES**

[1]     EN 1992-1-2, "Eurocode 2, Design of Concrete Structures, Part 1.2: General Rules - Structural Fire Design", Commission of the European Communities, Brussels, 2004.

[2]     EN 1994-1-2, "Eurocode 4, Design of Composite Steel and Concrete Structures, Part 1.2: General rules - Structural Fire Design", Commission of the European Communities, Brussels, 2005.

[3]      International Organisation for Standardisation, "ISO 834: Fire Resistance Tests - Elements of Building Construction", 1985.

[4]     Swinden Technology Centre, "The Behaviour of Multi-Storey Steel-Framed Buildings in Fire: A European Joint Research Programme", British Steel plc, Rotherham, UK, 1999.

[5]     Lie T.T., and Celikkod B., "Method to Calculate the Fire Resistance of Circular Reinforced Concrete Columns", *ACI Material Journal*, **88** (1), 1991, pp. 84-91.

[6]     Ellingwood B., and Lin T.D., "Flexure and Shear Behaviour of Concrete Beams during Fires", *Journal of Structural Engineering, ASCE*, **117**( 2), 1991, pp. 440-458.

[7]     Huang Z. and Platten A., "Non-linear Finite Element Analysis of Planar Reinforced Concrete Members Subjected to Fire", *ACI Structural Journal,* **94**(3), 1997, pp. 272-282.

[8]     Terro M. J., "Numerical Modeling of the Behavior of Concrete Structures in Fire", *ACI Structural Journal,* **95**(2), 1998, pp. 183-193.

[9]     Capua D. D. and Mari A. R., "Non-linear Analysis of Reinforced Concrete Cross-sections Exposed to Fire", *Fire Safety Journal,* **42**, 2007, pp. 139–149.

[10]    Bratina S., Saje M. and Planinc I., "The Effects of Different Strain Contributions on the Response of RC Beams in Fire" *Engineering Structures*, **29**, 2007, pp. 418-430.

[11]    Ngo D, Scordelis AC, "Finite Element Analysis of Reinforced Concrete Beams", *ACI Journal*, **64**(3), 1967, pp. 152-163.

[12]    Herrmann, L.R., "Finite Element Analysis of Contact Problems", *Journal of the Engineering Mechanics Division*, ASCE, **104**(EM5), Oct 1978, pp. 1043-1057.

[13]    Jendele, Libor and Cervenka, Jan, "Finite Element Modelling of Reinforcement with Bond", *Computer and Structures*, **84**, 2006, pp. 1780-1791.

[14]    Groot, A.K. De, Kusters, G.M.A., Monnier, Th., "Numerical Modelling of Bond-Slip Behavior," HERON, **26**(1B), 1981, 90 p.

[15]    Kwak, Hyo-Gyoung and Kim Sun-Pil, "Bond-slip Behaviour under Monotonic Uniaxial Loads", *Engineering Structures*, **23**, 2001, pp. 298-309.

[16]    Cruz, Jose Sena and Barros, Joaquim, "Modeling of Bond between Near-surface Mounted CFRP Laminate Strips and Concrete", *Computer and Structures*, **82**, 2004, pp. 1513-1521.

[17]    Schafer, H., "A Contribution to the Solution of Contact Problems with the Aid of Bond Elements," *Computer Methods in Applied Mechanics and Engineering*, **6**, 1975, pp. 335-354.

[18]    Keuser, M., Mehlhorn, G., "Finite Element Models for Bond Problems," Journal of Structural

Engineering, ASCE, **113**(10), Oct. 1987, pp. 2160-2173.

[19]  Mehlhorn, G., Kollegger, J., Keuser, M., Kolmar, W., "Nonlinear Contact Problems - A Finite Element Approach Implemented in ADINA," Computers and Structures, **21**(1-2), 1985, pp. 69-80,.

[20]  Allwood, R.J., Bajarwan, A.A., "A New Method for Modelling Reinforcement and Bond in Finite Element Analyses of Reinforced Concrete," International Journal for Numerical Methods in Engineering, **28**, 1989, pp. 833-844.

[21]  Cervera, M., Hinton, E., Hassan, O., "Nonlinear Analysis of Reinforced Concrete Plate and Shell Structures using 20-noded Isoparametric Brick Elements," Computers and Structures, **25**(6), 1987, pp. 845-869.

[22]  Huang, Z., Burgess, I. W. and Plank R. J., "3D Modelling of Beam-columns with General Cross-sections in Fire", Structures in Fire, Proceedings of the Third International Workshop, Ottawa, Canada, May 10-11 2004, pp. 323-334.

[23]  Huang, Z., Burgess, I. W. and Plank R. J., "Three-dimensional analysis of reinforced concrete beam-column structures in fire", Journal of Structural Engineering, ASCE, **135**(10), 2009, pp1201-1212.

[24]  CEB-FIP Model Code 90, First Draft, "Committee Euro-international du Beton, Bulletin d'information No. 195, 196", 1990.

[25]  Bazant, Z.P. and Kaplan, M.F., "Concrete at High Temperatures", Longman Group Limited, 1996.

[26]  Huang Z., Platten A. and Roberts J., "Non-linear Finite Element Model to Predict Temperature Histories within Reinforced Concrete in Fires", *Building and Environment*, **31**,(2), 1996, pp. 109-118.

[27]  Huang, Z., Burgess, I. W. and Plank R. J., "Influence of shear connectors on the behaviour of composite steel-framed buildings in fire", Journal of Constructional Steel Research, **51**(3), 1999, pp. 219-237.

[28]  Viwathanatepa, S., Popov, E.P., and Bertero V.V., "Seismic Behaviour of Reinforced Concrete Interior Beam-column Subassemblages", Report NO UCB/EERC-79/14, Earthquake Engineering Research Center, University of California, Berkeley, 1979.

[29]  Gaston, J.R., Siess, C.P., Newmark N.M., "A Layered Finite Element Non-linear Analysis of Reinforced Concrete Plates and Shells", Civil Engineering Studies, SRS No. 389, University of Illinois, Urbana, 1972.

[30]  Lin T. D., Ellingwood B. and Piet O., *"Flexural and Shear Behaviour of Reinforced Concrete Beams During Fire Tests"*, Report No. NBS-GCR-87-536, Center for Fire Research, National Bureau of Standards, 1987.
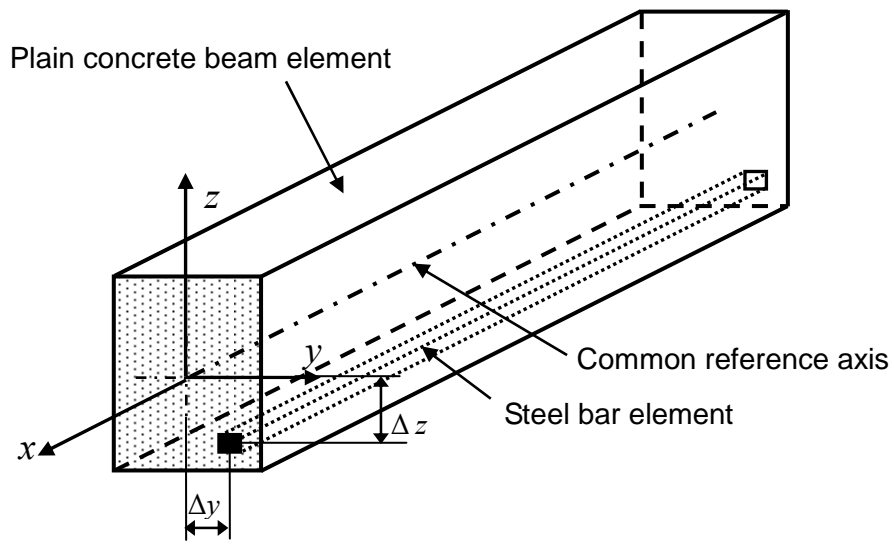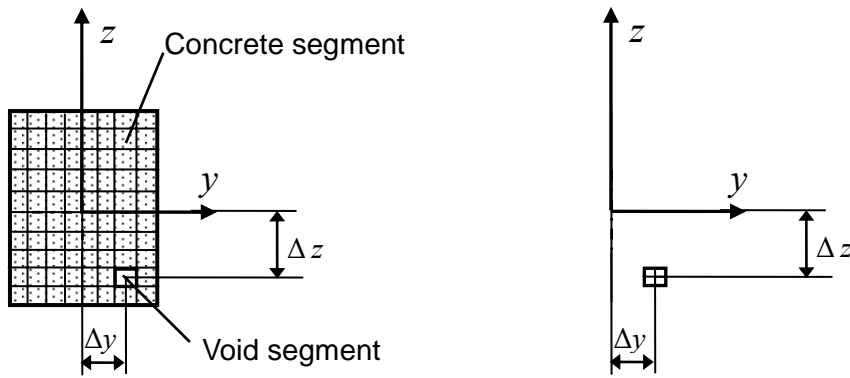
**FIGURES**

**List of Figures:**

Fig. 1   Reinforced concrete beam: plain concrete, reinforcing steel bar and bond-link elements.

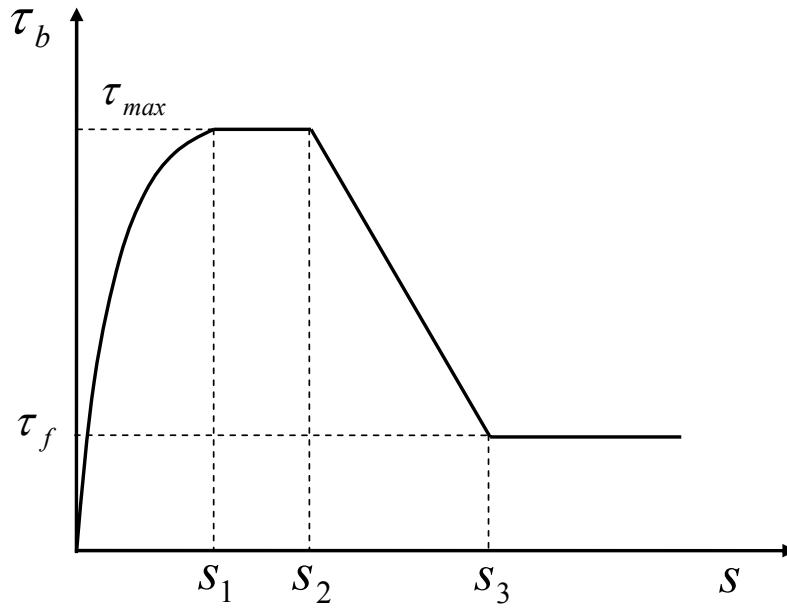Fig. 2   Segmentation of plain concrete beam and reinforcing steel bar elements.

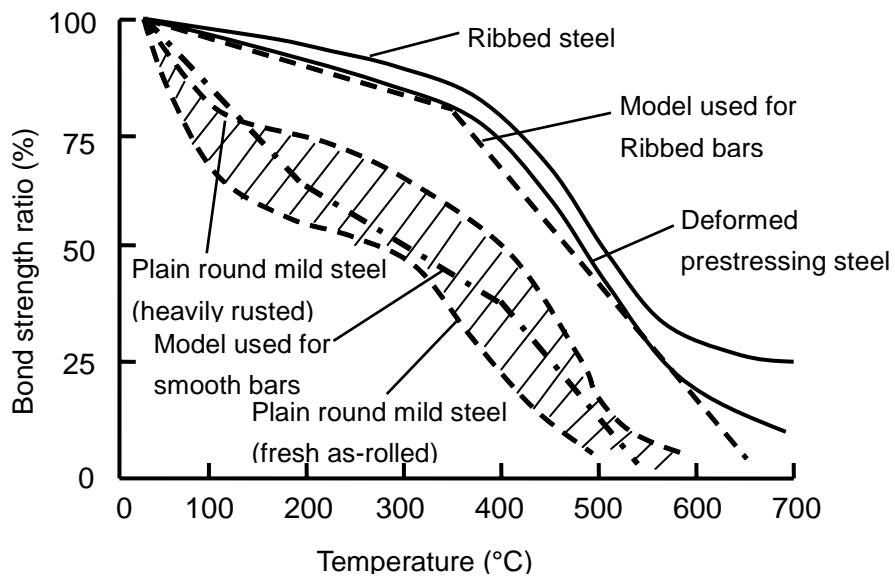Fig. 3   Bond stress-slip curve defined by CEB-FIP Model Code 1990 [24].

Fig. 4   Degradation of bond strength between concrete and reinforcing steel bar at elevated temperatures [25].

Fig. 5   An artificial simply supported reinforced concrete beam subject to transverse point load at centre.
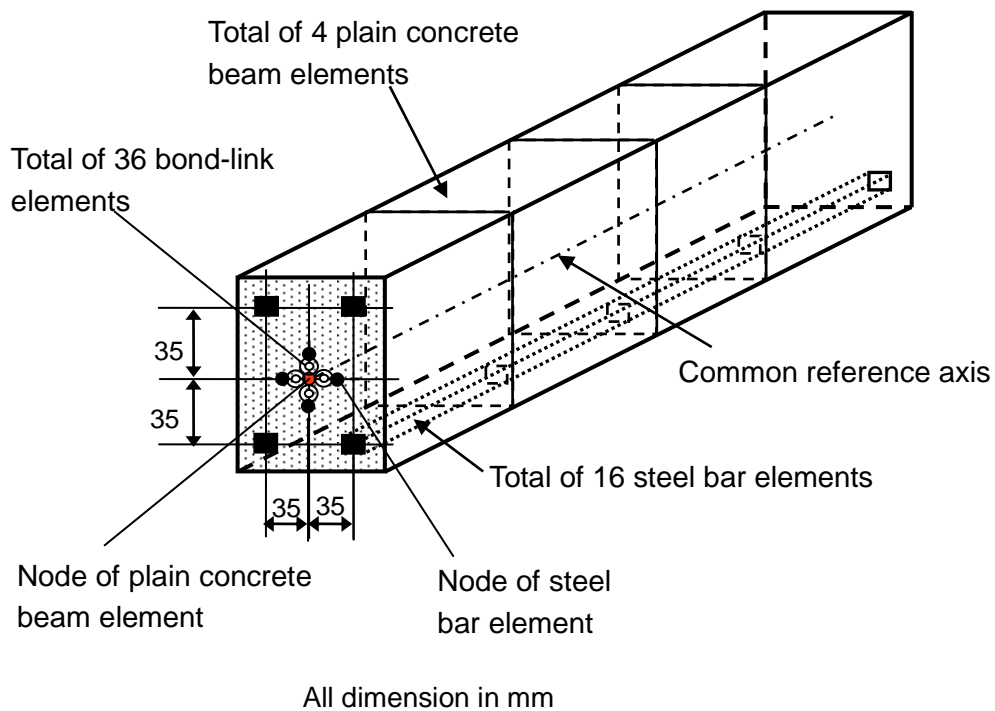
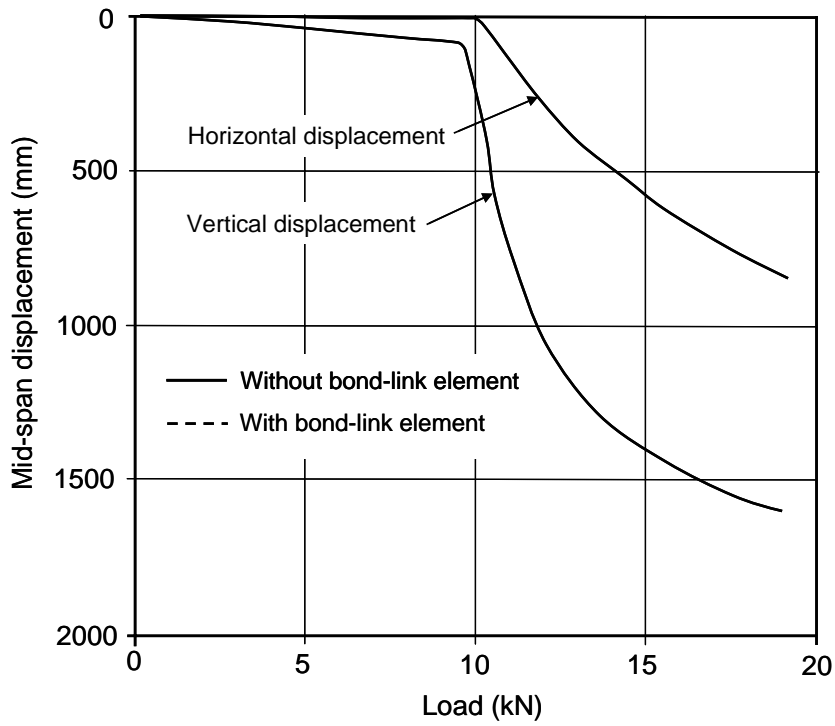Fig. 6   Finite element mesh for simply supported reinforced concrete beam.

Fig. 7   Comparison of predicted horizontal and vertical displacements at mid-span of the beam (modelled with and without bond-link element).
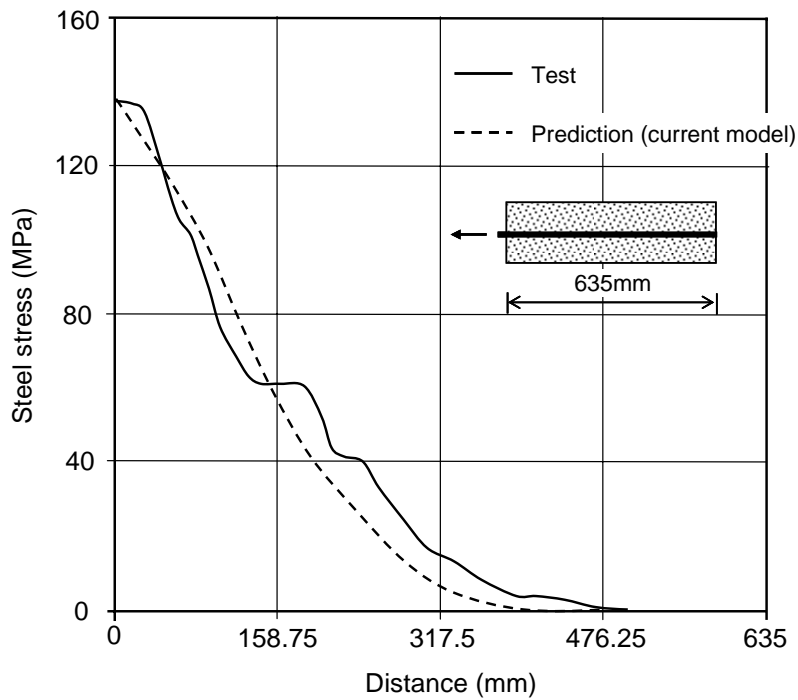
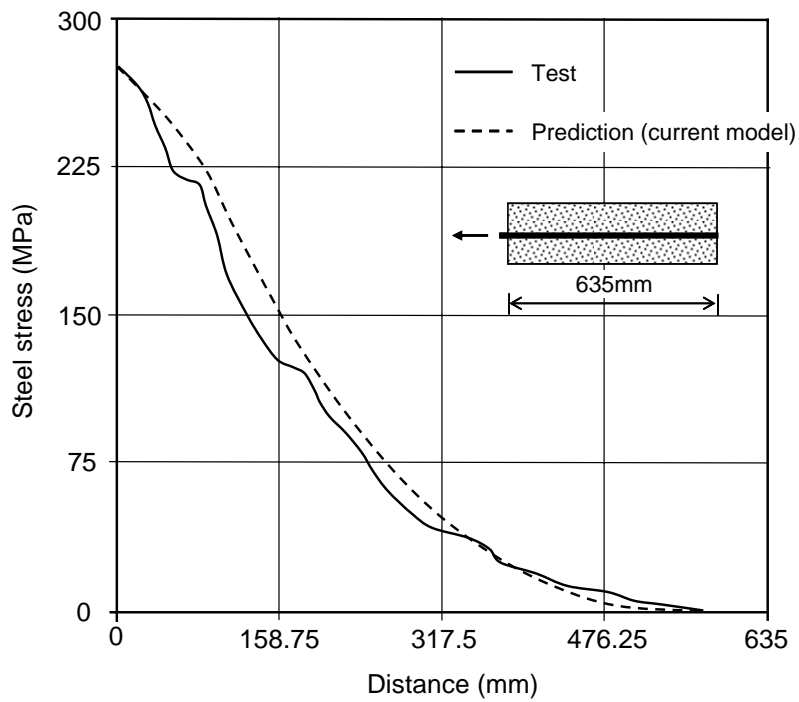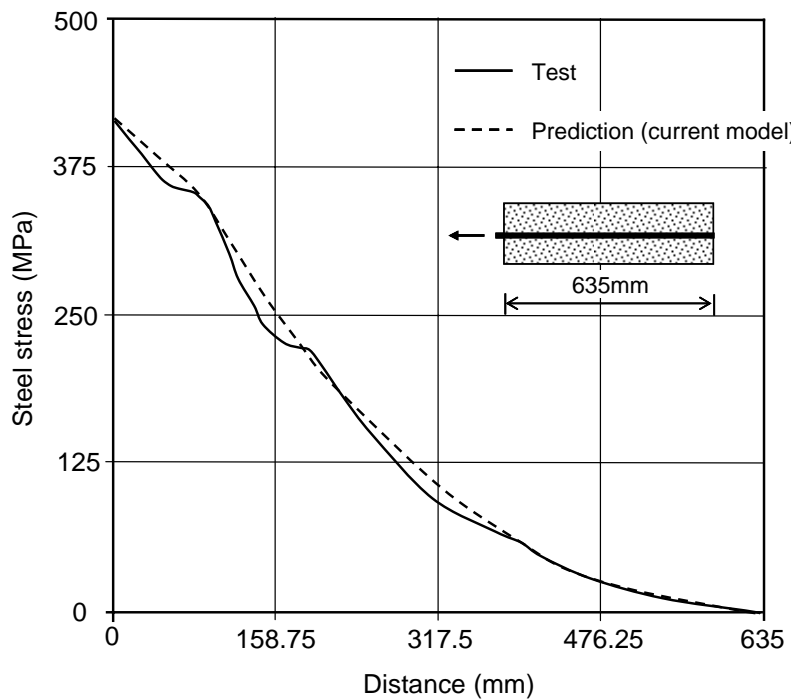Fig. 8   Comparison of predicted and measured stress distributions along anchored reinforcing steel bar [28]: (a) End stress = 138 MPa; (b) End stress = 276 MPa; (c) End stress =  414 MPa.
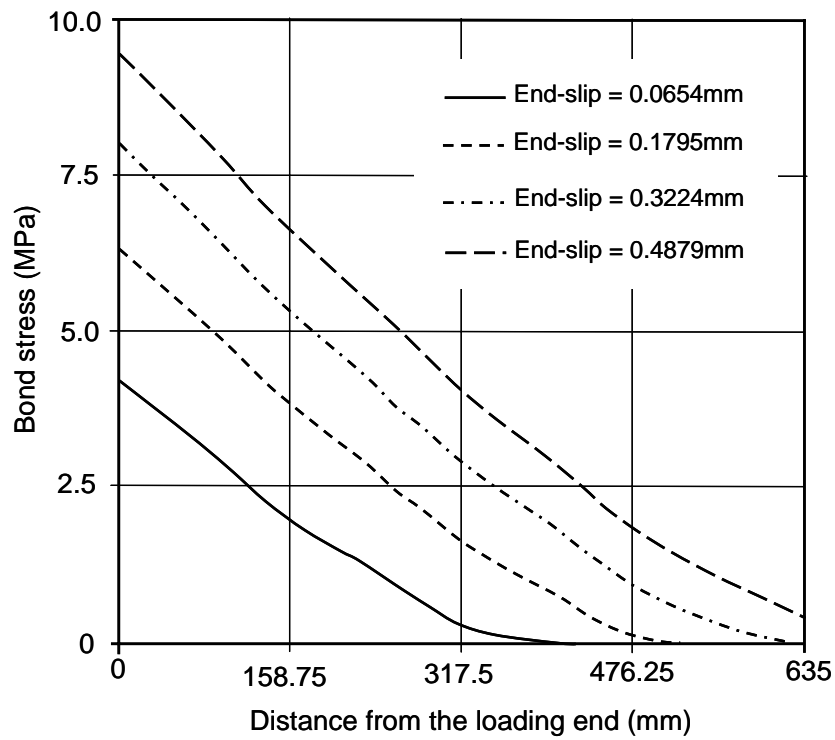
Fig. 9   Predicted bond stress distributions corresponding to different end-slips for the test [28].
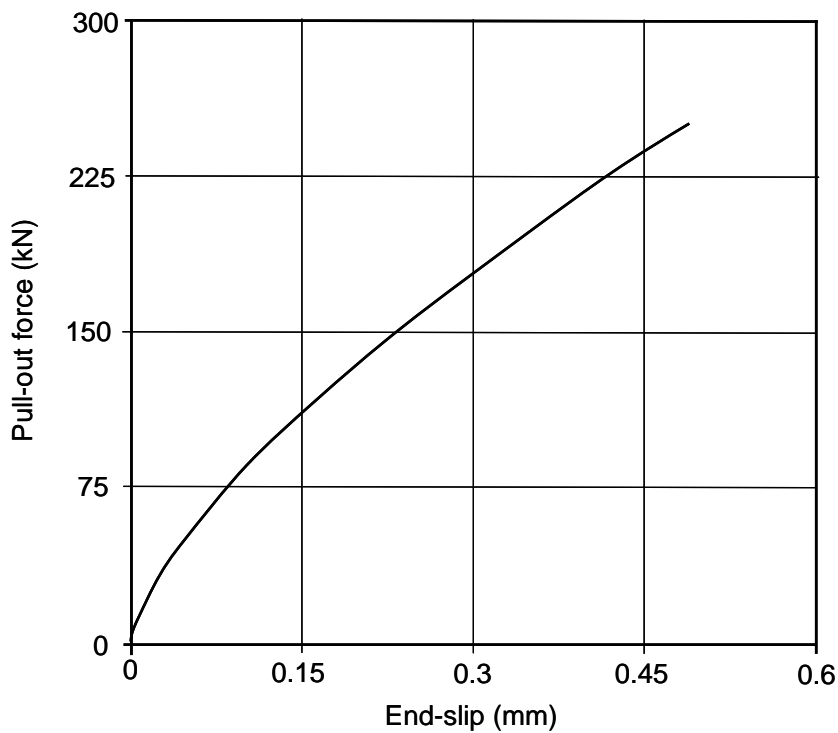
Fig. 10  Predicted end-slips against total pull-out force for the test [28].

Fig. 11  Details of tested beam at ambient temperature [29] used for comparison.

Fig. 12  Comparison of predicted and measured mid-span deflections of the tested beam [29].

Fig. 13  Details of tested beams in fires [30].

Fig. 14  Comparison of predicted and measured temperatures of four main reinforcing steel layers for Beam 1.

Fig. 15   Comparison of predicted and measured temperatures of four main reinforcing steel layers for Beam 5.

Fig. 16  Comparison of predicted and measured maximum deflections of Beam 1 (ASTM Fire).

Fig. 17  Comparison of predicted and measured maximum deflections of Beam 3 (ASTM Fire).

Fig. 18  Comparison of predicted deflections at the cantilever-end of Beam 3 (ASTM Fire).

Fig. 19  Comparison of predicted and measured maximum deflections of Beam 5 (SDHI Fire).

Fig. 20  Comparison of predicted and measured maximum deflections of Beam 6 (SDHI Fire).

Fig. 21  Comparison of predicted deflections at the cantilever-end of Beam 6 (SDHI Fire).

**(a)**



**(b)**

**Fig. 1** Reinforced concrete beam: plain concrete, reinforcing steel bar and bond-link elements.

**(a)**



**(b)**

**Fig. 2** Segmentation of plain concrete beam and reinforcing steel bar elements.

**Fig. 3** Bond stress-slip curve defined by CEB-FIP Model Code 1990 [24].



**Fig. 4** Degradation of bond strength between concrete and reinforcing steel bar at elevated temperatures [25].

P

4000mm

100mm

Reinforcing
Steel bars

100mm
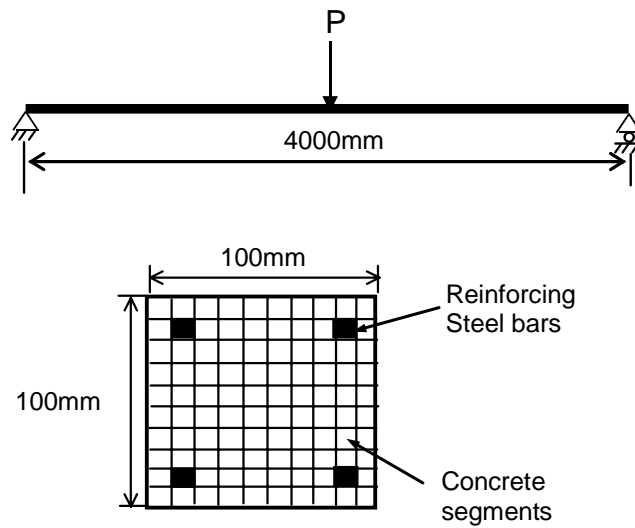
Concrete
segments

**Cross-section of the Beam**

**Fig. 5** An artificial simply supported reinforced concrete beam subject to transverse point load at centre.

Total of 4 plain concrete beam elements

Total of 36 bond-link elements

35

35

35 35

Common reference axis

Total of 16 steel bar elements

Node of plain concrete beam element

Node of steel bar element

All dimension in mm

**Fig. 6** Finite element mesh for simply supported reinforced concrete beam.

**Fig. 7**  Comparison of predicted horizontal and vertical displacements at mid-span of the beam (modelled with and without bond-link element).



**Fig. 8(a)**  Comparison of predicted and measured stress distributions along anchored reinforcing steel bar [28]: (a) End stress = 138 MPa;

24

**Fig. 8(b)** Comparison of predicted and measured stress distributions along anchored reinforcing steel bar [28]: (b) End stress = 276 MPa;



**Fig. 8(c)** Comparison of predicted and measured stress distributions along anchored reinforcing steel bar [28]: (c) End stress = 414 MPa.

**Fig. 9** Predicted bond stress distributions corresponding to different end-slips for the test [28].



**Fig. 10** Predicted end-slips against total pull-out force for the test [28].

26

**Fig. 11** Details of tested beam at ambient temperature [29] used for comparison.



**Fig. 12** Comparison of predicted and measured mid-span deflections of the tested beam [29].

**Fig. 13** Details of tested beams in fires [30].



**Fig. 14** Comparison of predicted and measured temperatures of four main reinforcing steel layers for Beam 1.

**Fig. 15** Comparison of predicted and measured temperatures of four main reinforcing steel layers for Beam 5.



**Fig. 16** Comparison of predicted and measured maximum deflections of Beam 1 (ASTM Fire).

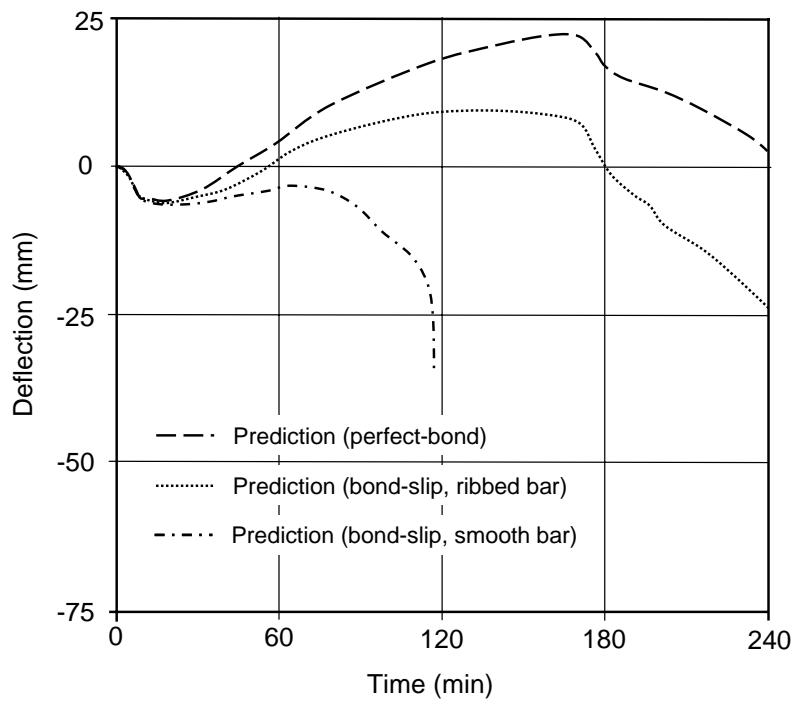**Fig. 17** Comparison of predicted and measured maximum deflections of Beam 3 (ASTM Fire).



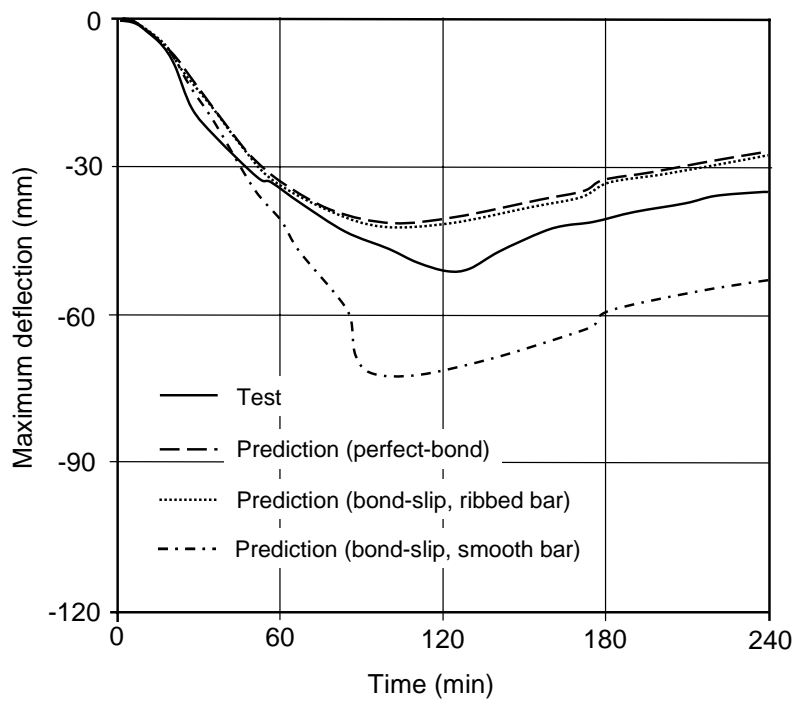**Fig. 18** Comparison of predicted deflections at the cantilever-end of Beam 3 (ASTM Fire).

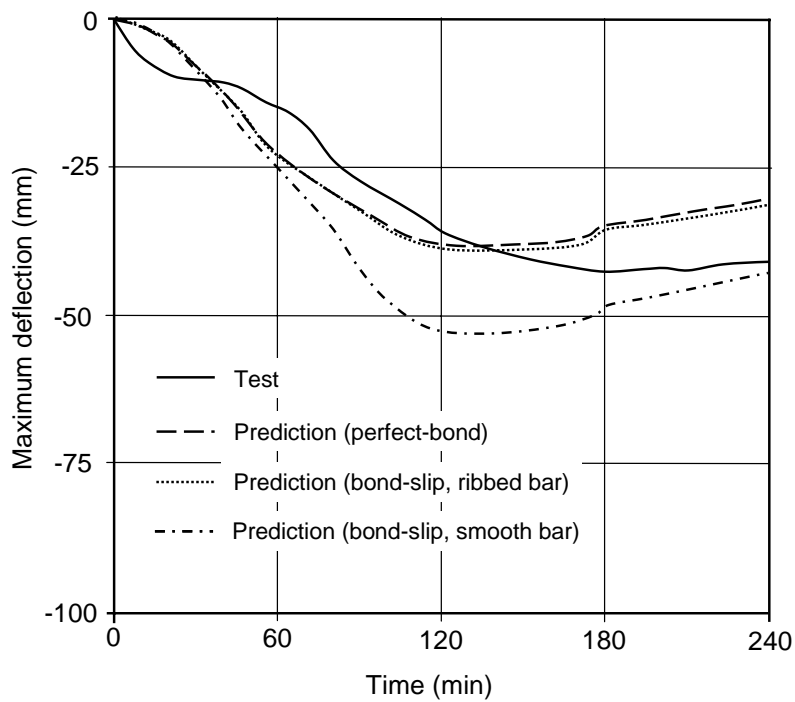**Fig. 19** Comparison of predicted and measured maximum deflections of Beam 5 (SDHI Fire).



**Fig. 20** Comparison of predicted and measured maximum deflections of Beam 6 (SDHI Fire).
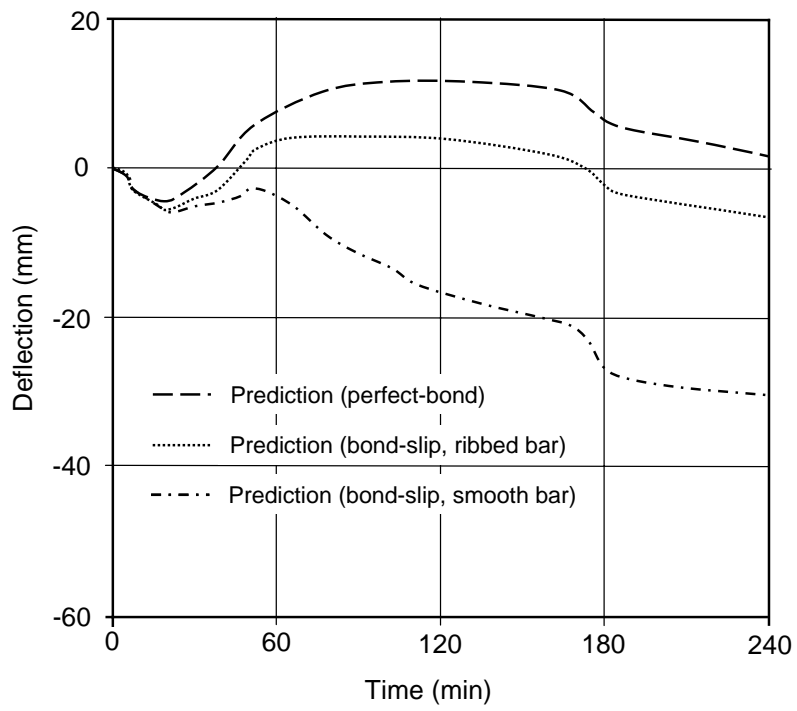
**Fig. 21** Comparison of predicted deflections at the cantilever-end of Beam 6 (SDHI Fire).